

# Upon viral exposure, myeloid and plasmacytoid dendritic cells produce 3 waves of distinct chemokines to recruit immune effectors

Bernard Piqueras, John Connolly, Heidi Freitas, Anna Karolina Palucka, and Jacques Banchereau

**Host response to viral infection involves distinct effectors of innate and adaptive immunity, whose mobilization needs to be coordinated to ensure protection. Here we show that influenza virus triggers, in human blood dendritic-cell (DC) subsets (ie, plasmacytoid and myeloid DCs), a coordinated chemokine (CK) secretion program with 3 successive waves. The first one, occurring at early time points (2 to 4 hours), includes CKs potentially**

**attracting effector cells such as neutrophils, cytotoxic T cells, and natural killer (NK) cells (CXCL16, CXCL1, CXCL2, and CXCL3). The second one occurs within 8 to 12 hours and includes CKs attracting effector memory T cells (CXCL8, CCL3, CCL4, CCL5, CXCL9, CXCL10, and CXCL11). The third wave, which occurs after 24 to 48 hours, when DCs have reached the lymphoid organs, includes CCL19, CCL22, and CXCL13, which at-**

**tract naive T and B lymphocytes. Thus, human blood DC subsets carry a common program of CK production, which allows for a coordinated attraction of the different immune effectors in response to viral infection. (Blood. 2006; 107:2613-2618)**

© 2006 by The American Society of Hematology

## Introduction

Upon microbial invasion, the immune system must first sense the microbe's presence and then rapidly deliver an appropriate response. This requires the precise coordination of several simultaneous tasks, including (1) influx of immediate immune effectors, such as neutrophils and natural killer (NK) cells, (2) activation of antigen-specific memory B and T lymphocytes into effector cells; and (3) priming of naive lymphocytes that leads to recruitment of more effector cells and, upon primary infection, establishment of immune memory. This complex program is thought to be coordinated by dendritic cells (DCs).<sup>1-3</sup>

DCs constitute a complex system of cells with common and unique functions. Human blood contains 2 DC subsets, myeloid (mDCs) and plasmacytoid (pDCs).<sup>3,4</sup> mDCs demonstrate remarkable plasticity and, depending on cytokine environment, can differentiate into either macrophages (with macrophage–colony-stimulating factor [M-CSF]), or distinct subsets of tissue-localized DCs, that is, epithelial Langerhans cells (with interleukin 15 [IL-15]) or transforming growth factor  $\beta$  [TGF- $\beta$ ] or interstitial DCs (with IL-4). Upon activation, mDCs secrete IL-12 and mature into antigen-presenting cells able to prime T cells. pDCs are considered poor antigen-presenting cells, but are major producers of type I interferons upon viral activation.<sup>5</sup>

DCs attract immune effectors through chemokines (CKs)<sup>6-9</sup> and regulate their maturation and function through cell-cell contact, and/or soluble factors.<sup>1-3</sup> Several studies analyzed CK secretion by DCs either generated *ex vivo* and exposed to bacterial products,<sup>10</sup> or sorted from the blood and exposed to influenza virus upon

culture with granulocyte macrophage–colony-stimulating factor (GM-CSF) and IL-4 (mDCs) or GM-CSF and IL-3 (pDCs).<sup>11,12</sup> Furthermore, secretion of a limited set of CKs was analyzed at a single time point after viral exposure.<sup>13</sup> Thus, there is a paucity of knowledge about the kinetics of CK response of primary blood DC subsets exposed to live influenza virus. As DCs need to coordinate the different steps of an immune response, we surmised that viral infection might trigger a sequential program of CK secretion that may permit such coordination.

## Materials and methods

### DC purification, staining and culture

pDCs and mDCs were purified from a healthy donor's buffy coats. Ficoll-enriched peripheral blood mononuclear cells (PBMCs) were depleted of lineage-positive cells with CD3, CD14, CD19, CD16, CD56, and glycoPhorin A microbeads (Miltenyi Biotec, Auburn, CA). After staining with lineage cocktail–fluorescein isothiocyanate (FITC), CD11c–allophycocyanin (APC) and CD123–phycoerythrin (PE; BD Biosciences, San Jose, CA) and HLA-DR-QR (Sigma, St Louis, MO) monoclonal antibodies (mAbs), cells were sorted on a FACSVantage (Becton Dickinson, San Jose, CA) to at least 99% purity.

For viral infection, purified pDCs and mDCs were cultivated in 96-well U-bottom plates (25 000 cells/well) in 200  $\mu$ L complete medium (RPMI 1640, 2 mM L-glutamine, penicillin/streptomycin, and 10% fetal calf serum), containing 1:125 hemagglutinin (HA) titer per milliliter of live influenza virus A/PR/8/34 (Charles River Laboratories, Wilmington, MA). At different time points cell pellets and supernatant were collected and stored at  $-80^{\circ}\text{C}$ .

From the Baylor NIAID (National Institute of Allergy and Infectious Disease) Cooperative Center for Translational Research on Human Immunology and Biodefense, and Baylor Institute for Immunology Research, Dallas, TX.

Submitted July 25, 2005; accepted November 10, 2005. Prepublished online as *Blood* First Edition Paper, November 29, 2005; DOI 10.1182/blood-2005-07-2965.

Supported by Baylor Health Care Systems (BHCS) foundation, DANA foundation, and the National Institutes of Health (U19 AIO57 234 and CA78 846). J.B. holds the Caruth Chair for Transplantation Immunology Research. A.K.P. holds the Ramsay Chair for Cancer Immunology Research.

J.B. and A.K.P. codirected this work.

The online version of this article contains a data supplement.

**Reprints:** Jacques Banchereau, BLIR, 3434 Live Oak, Dallas, TX 75204; e-mail: jacquesb@baylorhealth.edu; Bernard Piqueras, e-mail: piqueras@infobiogen.fr; or A. Karolina Palucka, e-mail: karolinp@baylorhealth.edu.

The publication costs of this article were defrayed in part by page charge payment. Therefore, and solely to indicate this fact, this article is hereby marked "advertisement" in accordance with 18 U.S.C. section 1734.

© 2006 by The American Society of Hematology

For phenotype analysis, DCs were stained as described in the first paragraph, but replacing the CD123-PE with CD123 biotin/streptavidin-Alexa Fluor 405 (Molecular Probes, Eugene, OR), sorted on a FACSAria (Becton Dickinson), and stained before or after influenza virus infection using PE-conjugated CD83, CD40 (Beckman Coulter); CD80, and CD86 (BD Biosciences).

### Microarray sample preparation and Genechip array hybridization

Cell pellets (250 000 cells) were resuspended in RLT buffer (Qiagen, Valencia, CA) and frozen at  $-80^{\circ}\text{C}$ . Total RNA was extracted with RNeasy columns (Qiagen), and analyzed with the 2100 Bioanalyser (Agilent, Palo Alto, CA). Amplification was as follows: total RNA (300 ng) was reverse transcribed for 2 hours at  $42^{\circ}\text{C}$  in the presence of 1  $\mu\text{M}$  T7-(dT)24 oligonucleotide (Operon, Huntsville, AL),  $1\times$  first strand buffer, 10 mM dithiothreitol (DTT), 0.75 mM deoxynucleoside triphosphate (dNTP), 20 U/ $\mu\text{L}$  Superscript II reverse transcriptase (all from Invitrogen, Carlsbad, CA), and 2 U/ $\mu\text{L}$  RNase inhibitor (Ambion, Austin, TX). Second strand synthesis was achieved by incubation for 2 hours at  $16^{\circ}\text{C}$ , after addition of  $1\times$  second strand buffer, 0.2 mM dNTP, 0.07 U/ $\mu\text{L}$  *Escherichia coli* DNA ligase, 0.27 U/ $\mu\text{L}$  *E coli* DNA polymerase I, 0.013 U/ $\mu\text{L}$  *E coli* RNase H, and then addition of 0.13 U/ $\mu\text{L}$  T4 DNA polymerase (all from Invitrogen) for 10 minutes at  $16^{\circ}\text{C}$ . Double-stranded cDNA was precipitated with 0.5 M ammonium acetate and 70% ethanol, and first round of in vitro transcription was performed for 6 hours at  $37^{\circ}\text{C}$ , in the presence of  $1\times$  Megascript buffer, 30 mM dNTP,  $1\times$  Megascript T7 enzyme mix (all from Ambion). Amplified cRNA was cleaned up using an RNeasy mini kit column (Qiagen), and quantified by migration on a 2100 Bioanalyser. Second reverse transcription was performed as for the first round but using 100 pM of a random hexamer pd(N)6 (Roche, Milan, Italy), and after treatment with 0.2 U/ $\mu\text{L}$  of RNase H at  $37^{\circ}\text{C}$  for 20 minutes and enzyme heat inactivation, second strand synthesis was performed by addition of 0.13  $\mu\text{M}$  T7-(dT)24 oligonucleotide,  $1\times$  second strand buffer, 0.2 mM dNTP, 0.27 U/ $\mu\text{L}$  *E coli* DNA polymerase I, and incubation at  $16^{\circ}\text{C}$  for 2 hours. Double-strand cDNA was then purified using the cDNA cleanup module from Affymetrix, and in vitro transcription was performed using the Enzo RNA transcript labeling kit (Affymetrix, Santa Clara, CA). Finally, biotin-labeled cRNA was purified using the cRNA cleanup module (Affymetrix), and stored at  $-80^{\circ}\text{C}$  until hybridization. Purified biotin-labeled cRNA was then fragmented and hybridized on the human Genechip expression arrays U133 A and B (Affymetrix), according to protocols provided by the manufacturer.

### Microarray data analysis

Raw intensity values from each chip were first prescaled to the 500 target intensity value in Affymetrix Microarray suite (MAS 5.0), before being imported in GeneSpring 6.1 (Silicon Genetics, Santa Clara, CA). Chip quality was evaluated by analyzing variability within the parameters of MAS expression report: scale factor, average background, percentage of present calls, 3' bias for GAPDH (glyceraldehyde-3-phosphate dehydrogenase) and actin, and spike control expression; we verified that the value for each chip was included within the mean plus or minus 2 standard deviations. In GeneSpring, for per chip normalization, each measurement on each chip was normalized to the 50th percentile of the measurements on that chip; for per gene normalization, the measurement of each probe was normalized to the median of the measurements of that probe in the different chips. Before applying any statistical test, the normalized intensities were then log transformed, and gene lists were filtered, first on flags, excluding genes that were called absent in all chips, and then on confidence using a *t* test *P* value with no multiple testing correction, selecting genes whose expression was varying significantly across the experiment. Finally, samples were grouped by conditions (pDCs versus mDCs, and noninfected versus virus infected), for statistical group comparison using analysis of variance test (ANOVA) with a Bonferroni multiple testing correction. To analyze gene expression of selected gene list, chips were normalized with a per chip normalization without any per gene normalization or any log transformation. We thus arbitrarily considered as significantly expressed genes whose normalized intensity was 3 times higher than the 50th percentile.

### Luminex and ELISA

CXCL8, CCL3, CCL4, CCL5, CXCL9, and CXCL10 were assessed by Luminex (Biosource). Samples were treated according to manufacturer's protocols. CCL19, CCL22, CXCL1, CXCL13, and CXCL16 expression was analyzed by enzyme-linked immunosorbent assay (ELISA; R&D Systems, Minneapolis, MN). All samples were treated in duplicates according to the manufacturer's protocol.

### Cell-migration experiments and analysis

Cell migration experiments were performed by placing 29  $\mu\text{L}$ /well of DCs culture supernatant, in 96-well ChemoTX lower plates (Neuroprobe, Gaithersburg, MD); and  $150\times 10^3$  PBMCs per well on the top of the ChemoTX membrane (5.7-mm diameter, 3- $\mu\text{m}$  pore size). After 45 minutes at  $37^{\circ}\text{C}$  with 5%  $\text{CO}_2$ , adherent cells on the bottom of the membrane were detached. After incubation at  $4^{\circ}\text{C}$  for 30 minutes, plates were centrifuged and cells were pooled and stained with CD3-PERCP, CD4-APC, CD8-APC, CCR7-PE, and CD45RA-FITC mAbs to analyze T-lymphocyte migration; CD19-APC, CD27-PE, and anti-IgD-FITC (Dako, Glostrup, Denmark) to analyze B-cell migration; CD16-FITC, CD14-PE, CD3-PERCP, and CD56-APC mAbs to analyze monocyte, macrophage, NK, and NKT cell migration; LIN-FITC, HLA-DR-PERCP, CD11c-APC, and CD123-PE mAbs, to analyze DC migration. All mAbs were from BD Biosciences. Statistical comparison of cell migration was done using 2-tailed paired *t* test.

## Results

### Influenza virus triggers a common CK production program in human pDCs and mDCs

To determine the global CK production program triggered in human DC subsets upon viral exposure, we used gene microarray analysis in mDCs and pDCs purified from 6 healthy donors, before and 24 hours after in vitro exposure to influenza virus (Influenza A/PR/8/34). Statistical comparison and analysis of fold-change expression values showed that influenza virus up-regulated 4712 probe sets in pDCs and 4560 probe sets in mDCs (data not shown). Twenty of these differentially expressed transcripts encoded CKs (Figure 1A), leading us to carry out a systematic analysis of influenza virus-induced CK transcript expression in mDCs and pDCs (44 CK probe sets were present on the U133 chips). Transcripts with expression levels at least 3-fold over the 50th percentile were considered significant (Figure 1B). Thus, 4 of 44 CKs were significantly expressed in both DC subsets before activation (*CXCL4*, *CXCL7*, *CXCL8*, and *CXCL16*; Figure 1B-C). mDCs expressed more *CXCL8* ( $\times 7$ ) and *CXCL16* ( $\times 36$ ) than pDCs, whereas levels of *CXCL4* and *CXCL7* were comparable (Figure 1B-C and Table S1, which is available on the *Blood* website; see the Supplemental Materials link at the top of the online article). Moreover, mDCs, which displayed a more activated phenotype based on CD86, CD83, and HLA-DR expression (Figure S1), also expressed *CCL3* and *CXCL2*. *CXCL4* is a major product of platelets<sup>14-16</sup> previously not identified in DCs. Although the lack of reagents does not permit demonstration of the production of *CXCL4* by DCs, the purity of DC preparations determined by FACS analysis and the absence of platelet-specific gene expression exclude a possible platelet contamination.

Upon exposure to influenza virus for 24 hours, expression of these 4 CKs was reduced and 12 others were turned on in both pDCs and mDCs (Figure 1B-C; Table S1). These included CKs attracting polymorphonuclear cells (PMNCs): *CXCL1*, *CXCL2*, and *CXCL3*<sup>17</sup>; CKs involved in the inflammatory response: *CCL3*, *CCL4*, and *CCL5*<sup>17,18</sup>; interferon-inducible CKs *CXCL9*, *CXCL10*,

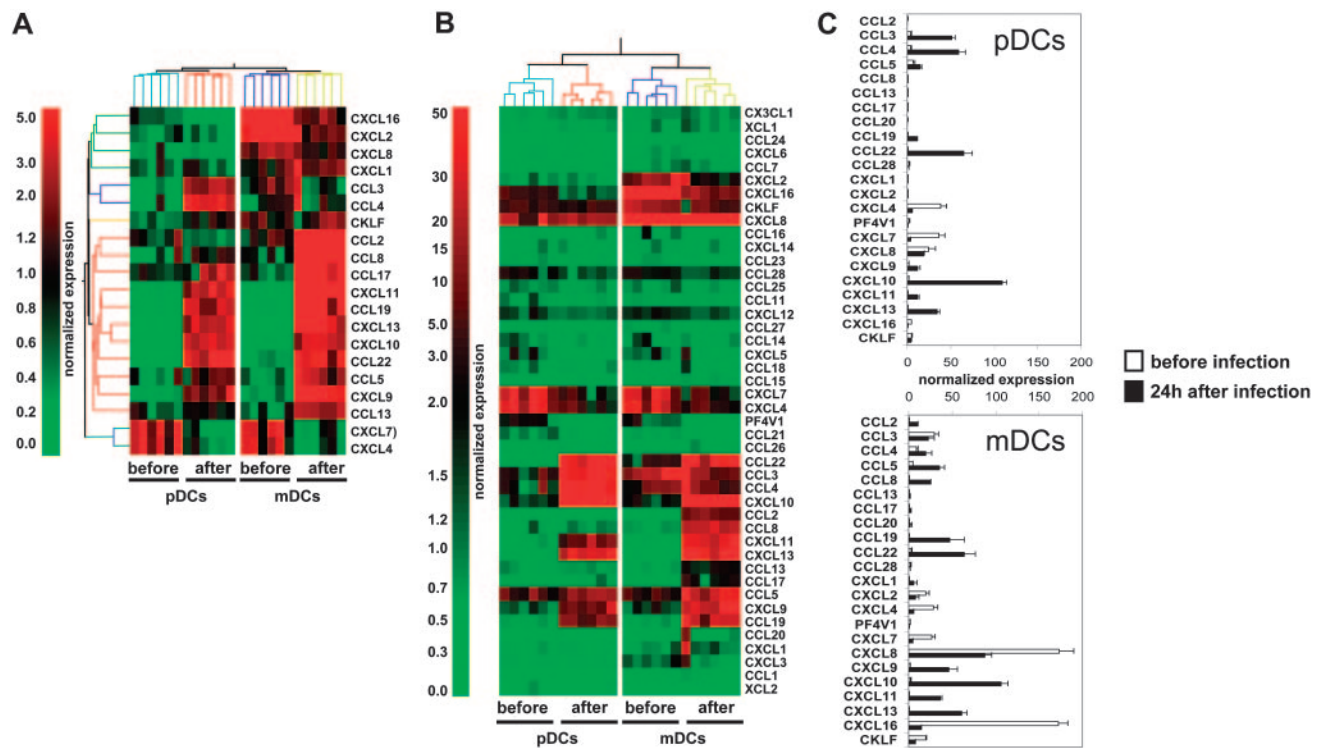


**Figure 1. Transcription of CK genes in blood DC subsets exposed to influenza virus.** (A) Total RNA was extracted from pDCs and mDCs of 6 healthy donors after sort (before), and of 6 other donors 24 hours after culture with influenza virus (after). Amplified cRNA was hybridized on Affymetrix HG-U133 chips. Gene expression was analyzed with GeneSpring 6.1 software. Each probe set was normalized with a per chip normalization to the 50th percentile, and a per gene normalization to the median of each gene. Within the most differentially expressed probe sets ( $P < .05$  with Bonferroni multiple testing correction, or  $> 2$  fold-change), we identified a set of 20 chemokine probes. (B) Transcription of 44 different chemokines. After per-chip normalization to the 50th percentile, the normalized intensity values of each probe set were used as a measurement of its expression. (C) Normalized expression of the most significantly transcribed chemokines (3-fold over the 50th percentile). Each bar is representative of mean normalized intensity plus or minus standard error for chemokine's gene expression in pDCs and mDCs from 6 healthy donors before infection or 6 healthy donors after infection.

and *CXCL11*<sup>17</sup>; as well as CKs expressed in lymphoid tissues *CCL19*, *CCL22*, and *CXCL13*.<sup>17</sup> The spectrum of CKs induced by influenza virus exposure was remarkably similar between the 2 DC subsets. Only 2 of 44 CK transcripts, the monocyte-attracting CKs *CCL2* and *CCL8*,<sup>17</sup> were uniquely expressed in mDCs. The comparative analysis of the 2 DC subsets showed that mDCs expressed higher levels of *CCL5* ( $\times 2.4$ ), *CXCL9* ( $\times 3.8$ ), *CXCL11* ( $\times 3.1$ ), *CCL19* ( $\times 4.3$ ), and *CXCL13* ( $\times 1.8$ ); whereas pDCs expressed higher levels of the inflammatory CKs *CCL3* ( $\times 2.3$ ), and *CCL4* ( $\times 3$ ).

#### Influenza virus triggers a coordinated CK production program with 3 successive waves

To analyze the kinetics of CK expression, purified DCs (25 000 cells) were exposed to influenza virus (1/125 HA titer per  $\mu\text{L}$ ); pellets and supernatants were collected at 4, 8, 16, 24, and 48 hours (Figure 2). Before viral exposure, *CXCL4* and *CXCL16* were actively transcribed in both subsets (Figure 2A-B). The *CXCL16* protein was, however, detected in mDC but not pDC supernatants (Figure 2D). *CXCL16*, which, like *CX3CL1*, is expressed as a transmembrane protein,<sup>19</sup> is cleaved by a metalloprotease and attracts effector cells expressing the *CXCR6* receptor.<sup>20,21</sup> The expression of *CXCL4* has been found earlier in platelets<sup>14,15</sup> and monocytes.<sup>22</sup> The transcription of both *CXCL4* and *CXCL16* is down-regulated upon viral exposure.

In the early postviral exposure phase, 2 to 4 hours, DCs transcribe mainly *CXCL1*, *CXCL2*, *CXCL3*, and *CXCL8*, which

are known to attract PMNCs.<sup>23</sup> The peak of their transcription occurred approximately 2 hours after exposure and subsequently decreased (Figure 2E-F). *CXCL8* protein could be detected in supernatants of both pDCs and mDCs 4 hours after exposure, and reached a maximum at 12 hours (Figure 2G-H).

At intermediate phase (4 to 8 hours) after viral exposure, the transcription of the inflammatory CKs *CCL3*, *CCL4*, and *CCL5* (Figure 2I-J) and the interferon-regulated CKs *CXCL9*, *CXCL10*, and *CXCL11* was induced in both mDCs and pDCs (Figure 2M-N). Transcription of these genes reached its peak at 8 hours, while corresponding protein expression was detected in supernatants at 12 hours for *CCL3* and *CCL4* (Figure 2K-L), and 24 hours for *CCL5*, *CXCL9*, and *CXCL10* (Figure 2K-L, O-P). All of the CKs produced at the intermediate time points are known to attract activated memory T cells.<sup>24</sup> Furthermore, the CKs *CCL3*, *CCL4*, and *CCL5*, are chemotactic for *CCR5* expressing monocytes and DCs.<sup>18</sup>

Finally, at late time points ( $> 12$  hours after exposure), *CCL19*, *CCL22*, and *CXCL13* transcripts were expressed by both pDCs and mDCs (Figure 2Q-R). The CKs could be detected in supernatants 24 to 48 hours after viral exposure (Figure 2S-T). These CKs attract lymphocytes. *CCL19* is chemotactic for *CCR7*-expressing cells,<sup>25</sup> that is, naive and central memory T cells (*CD45RA*<sup>+/−</sup>, *CCR7*<sup>+</sup>),<sup>26,27</sup> as well as mature DCs.<sup>28,29</sup> *CCL22* attracts Th2 effector memory T cells.<sup>30</sup> *CXCL13* is the main CK responsible for B-cell attraction.<sup>31,32</sup> Finally, 2 monocyte chemoattractants, *CCL2* and *CCL8*, were expressed predominantly by mDCs (Figure 2U-X). Interestingly, we did not observe *CCL17* expression by mDCs, which seems in contrast to an earlier study.<sup>11</sup> A possible

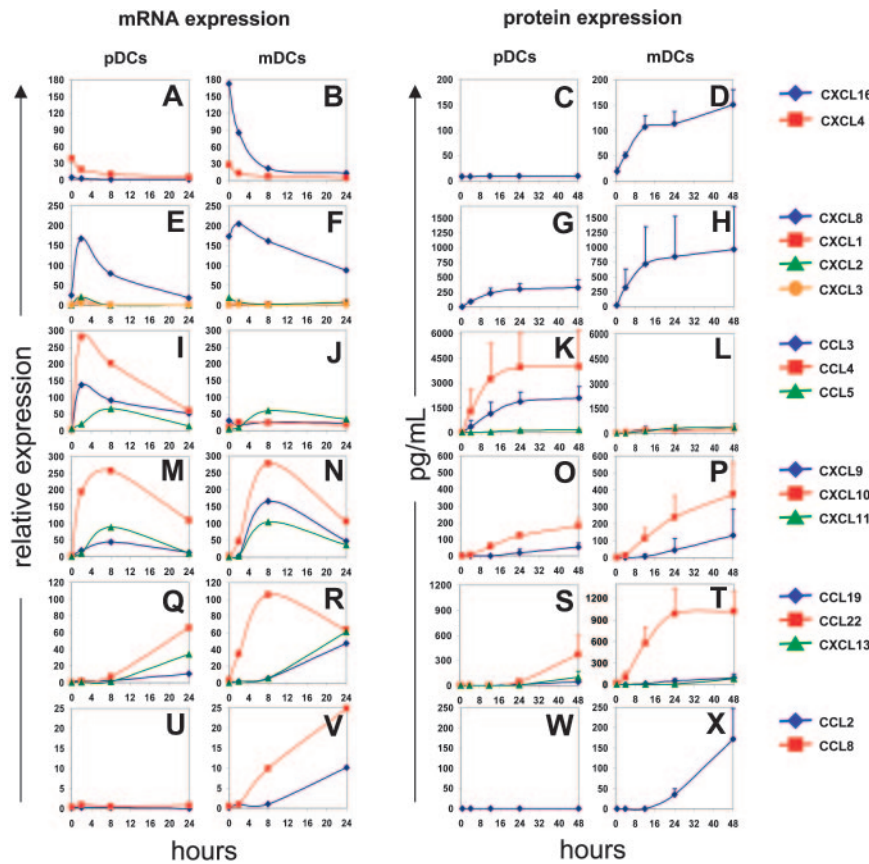


**Figure 2. Kinetics of CK expression.** Blood DCs isolated from 4 donors were exposed to influenza virus. Total RNA was processed and gene expression was analyzed after per chip normalization as in Figure 1 (left). Protein expression was evaluated by multiplex cytokine analysis (Luminex; CCL2, CCL3, CCL4, CCL5, CXCL8, CXCL9, and CXCL10) or by ELISA (CXCL16, CCL19, CCL22, and CXCL13) (right). CXCL16 and CXCL4 are expressed before infection and their expression constantly decreases upon viral stimulation (A-D). CXCL1, CXCL2, CXCL3, and CXCL8 are transiently expressed between 2 and 8 hours, longer for CXCL8 (E-H). Inflammatory chemokines (CCL3, CCL4, CCL5) and interferon-dependent chemokines (CXCL9, CXCL10, CXCL11) expression is up-regulated between 2 and 8 hours and then decreases progressively (I-P). CCL19, CCL22, and CXCL13 are significantly expressed after 8 to 24 hours (Q-T). Finally, CCL2 and CCL8 are expressed only by infected mDCs (U-X).

explanation might come from different experimental approaches, with different methods to isolate mDCs and activation using another strain of inactivated influenza virus.

**Influenza virus–triggered DC subsets attract monocytes, NK cells, and effector memory CD4<sup>+</sup> T cells**

We next analyzed the attraction of different immune effectors using an in vitro migration assay. Supernatants of DC subsets, exposed to influenza virus for 24 hours, were added to the lower part of a migration chamber. PBMCs, isolated from 4 healthy volunteers, were added on top of a 3- $\mu$ m pore diameter filter. Migration of

different immune cells was analyzed by viable cell count and flow cytometry after a 45-minute incubation to determine which immune effectors are attracted in the early phase after viral exposure. As shown in Figure 3A, supernatants of DCs exposed to influenza virus attracted more PBMCs (mean  $\pm$  SD =  $587 \times 10^3 \pm 181 \times 10^3$  for pDCs and  $344 \times 10^3 \pm 99 \times 10^3$  for mDCs;  $P = .009$  and  $.002$ , respectively;  $n = 4$ ) than culture medium containing influenza virus (mean  $\pm$  SD =  $121 \times 10^3 \pm 67 \times 10^3$ ). Supernatants of pDCs attracted more PBMCs than supernatants of mDCs ( $P = .04$ ). These results indicate that DCs exposed to influenza virus attract PBMCs. To determine which cells were actually

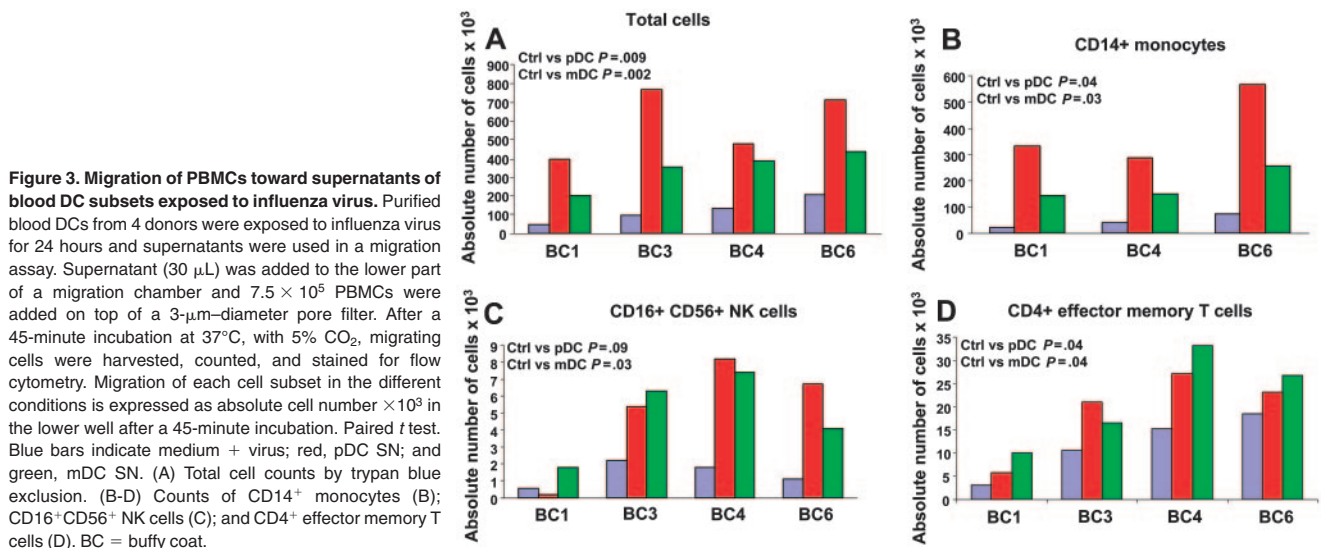


**Figure 3. Migration of PBMCs toward supernatants of blood DC subsets exposed to influenza virus.** Purified blood DCs from 4 donors were exposed to influenza virus for 24 hours and supernatants were used in a migration assay. Supernatant (30  $\mu$ L) was added to the lower part of a migration chamber and  $7.5 \times 10^5$  PBMCs were added on top of a 3- $\mu$ m-diameter pore filter. After a 45-minute incubation at 37°C, with 5% CO<sub>2</sub>, migrating cells were harvested, counted, and stained for flow cytometry. Migration of each cell subset in the different conditions is expressed as absolute cell number  $\times 10^3$  in the lower well after a 45-minute incubation. Paired *t* test. Blue bars indicate medium + virus; red, pDC SN; and green, mDC SN. (A) Total cell counts by trypan blue exclusion. (B-D) Counts of CD14<sup>+</sup> monocytes (B); CD16<sup>+</sup>CD56<sup>+</sup> NK cells (C); and CD4<sup>+</sup> effector memory T cells (D). BC = buffy coat.

attracted, cells from lower wells were analyzed with a panel of monoclonal antibodies that identify monocytes, DC subsets, NK cells, CD4<sup>+</sup> and CD8<sup>+</sup> T cells and their subsets, as well as B cells. As shown in Figure 3B, CD14<sup>+</sup> monocytes represented the largest number within migrating PBMCs ( $393 \times 10^3 \pm 150 \times 10^3$  for pDCs and  $183 \times 10^3 \pm 64 \times 10^3$  for mDCs;  $P = .04$  and  $.03$ , respectively;  $n = 3$ ) as compared with control ( $44 \times 10^3 \pm 26 \times 10^3$ ). In 4 of 4 donors analyzed, mDC supernatants attracted significant numbers of CD3<sup>-</sup>CD16<sup>+</sup>CD56<sup>+</sup> NK cells ( $4.9 \times 10^3 \pm 2.5 \times 10^3$  for mDCs and  $1.4 \times 10^3 \pm 0.7 \times 10^3$  for control medium;  $P = .03$ ;  $n = 4$ ; Figure 3C). pDC supernatants significantly attracted NK cells in 3 donors ( $6.75 \times 10^3 \pm 1.4 \times 10^3$  for pDCs and  $1.7 \times 10^3 \pm 0.6 \times 10^3$  for control medium;  $P = .03$ ;  $n = 3$ , BC3, 4, and 6; Figure 3C). Finally, the analysis of T-cell subsets in migrating PBMCs revealed increased numbers of CD4<sup>+</sup> T cells with effector memory phenotype (CD3<sup>+</sup>CD4<sup>+</sup>CD45RA<sup>-</sup>CCR7<sup>-</sup>;  $19 \times 10^3 \pm 9 \times 10^3$  for pDCs,  $22 \times 10^3 \pm 10 \times 10^3$  for mDCs, and  $12 \times 10^3 \pm 7 \times 10^3$  for control medium;  $P = .04$ ;  $n = 4$ ; Figure 3D). These results suggest that early after exposure to virus, both mDCs and pDCs attract innate immune effectors and effector memory CD4<sup>+</sup> T cells.

## Discussion

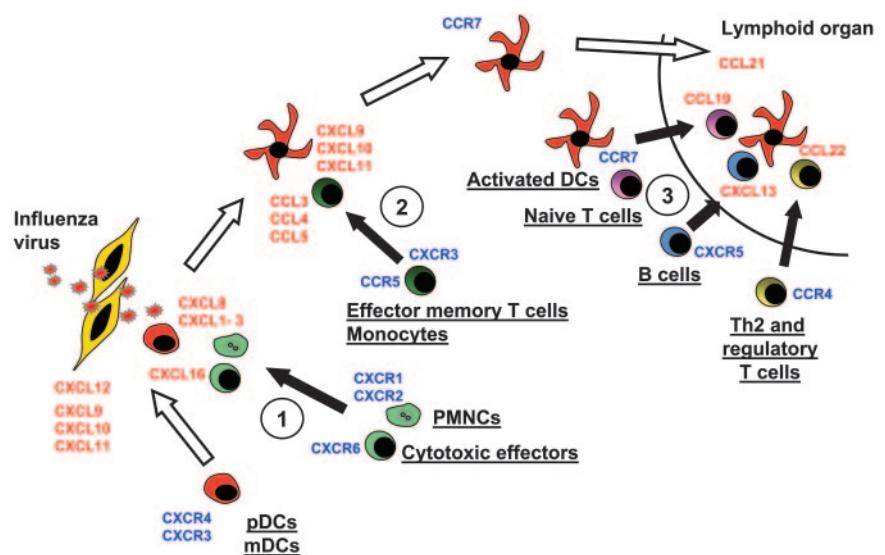
Our results demonstrate that upon exposure to live influenza virus, freshly isolated blood mDCs and pDCs produce 3 waves of CKs, which allow attraction of immune effectors. Although pDCs and mDCs strikingly differ in their biology, they display a remarkably similar pattern of CK secretion despite some qualitative (CCL2, CCL8, and CXCL16 expressed in mDCs only) and quantitative (CCL3, CCL4, and CCL5 expressed at higher levels in pDCs) differences. Such a sequential CK secretion program might actually explain how the DCs coordinate immune responses as they mature and migrate toward lymphoid organs (Figure 4). Interestingly, this sequential CK program is reminiscent of the sequential CK secretion triggered by lipopolysaccharide (LPS) in cultured DCs.<sup>10</sup> These results suggest that the various DC subsets share a common program to attract immune effectors.

Thus, the first-produced CKs are those attracting innate effectors and cytotoxic cells, which might limit the spread of infection. The next wave involves CKs that attract memory T cells and those

that attract monocytes, which could replenish the pool of DCs or tissue macrophages. Finally, as mature DCs land in the secondary lymphoid organs they secrete CKs that attract B cells and naive T cells, allowing their priming. Attraction of T cells with regulatory/suppressor function might finally permit the termination of immune response. Accordingly, CXCL13 has been shown to attract B cells as well as CXCR5<sup>+</sup>CD4<sup>+</sup> memory T cells that can enhance IgG and IgA production.<sup>32</sup> Furthermore, CXCL13-producing cells are located uniquely in the follicles and germinal centers.<sup>31</sup> Thus, influenza virus-activated blood DCs that migrate to B-cell areas of peripheral lymphoid organs could launch humoral immunity via CXCL13. Influenza-activated DCs that migrate to the T-cell zone could launch T-cell immunity via CCL19 and CCL22. Indeed, both chemokines are expressed by mature DCs in the T-cell areas.<sup>26,33</sup> CCL19 is chemotactic for CCR7 expressing naive and central memory T cells,<sup>26,27</sup> whereas CCL22 is chemoattractant for Th2 effector memory T cells.<sup>30</sup>

It is intriguing that each wave is composed of several CKs with similar functions. Recent studies have demonstrated that CKs act in synergy, where one CK would sensitize the cells to another, thereby amplifying the attraction of immune effectors.<sup>34,35</sup> Furthermore, the production of several CKs able to attract the same type of immune cells might represent a mechanism to compensate for the CK antagonists that viruses have created during their evolutionary fight against the immune system. For example, the poxviruses and herpes viruses evolved several means to compromise the CK network.<sup>36,37</sup> These include secretion of CK binding proteins that compete with CKs secreted by host cells (reviewed in Seet and McFadden<sup>36</sup>). Immature/nonactivated DCs patrolling via blood could be attracted to the site of pathogen entry in a process mediated via their expression of CXCR3 and CXCR4. The respective ligands are secreted by epithelial cells upon virus entry. Indeed, McWilliam et al<sup>38</sup> found that DCs are the first to arrive at the site of pathogen entry, preceding even neutrophils, a finding consistent with our model. Furthermore, we have found that both mDCs and pDCs are attracted *in vivo* to the respiratory tract in children with acute viral infections triggered by influenza virus or respiratory syncytial virus (RSV). Upon influenza exposure, the down-regulation of CXCR4 expression and up-regulation of CCR7 expression (data not shown) would allow the migration of pDCs and mDCs into lymphoid organs where, by production of appropriate CKs, they would launch immune response. This coordinated program of successive waves of CK production triggered by viral exposure in

**Figure 4. Model of DC migration and sequential effector-cell attraction.** Blood DCs expressing, at the steady state, CXCR4 and CXCR3, can migrate through virally infected tissues, expressing CXCL12, CXCL9, CXCL10, and CXCL11. There, they can penetrate the tissues. Upon encountering the virus, they start to release at the first step CXCL16, CXCL1, CXCL2, CXCL3, CXCL7, and CXCL8. These CKs attract Th1 effector cells expressing CXCR6 and neutrophils expressing CXCR2 (no. 1 in figure). Later, activated DCs secrete CCL2, CCL3, CCL4, CCL5, and CCL8, which essentially attract CCR5-expressing memory T lymphocytes and monocytes (no. 2). Upon maturation, DCs up-regulate CCR7 and down-regulate CXCR4, allowing, with L-selectin expression, their migration to high endothelial venules expressing CCL21 in lymphoid organs. In the T-cell area, activated pDCs secrete CCL19 and CXCL13, which respectively attract CCR7-expressing naive T cells and CXCR5-expressing naive B cells (no. 3). They also secrete CCL22, attracting CCR4-expressing Th2 and CD4<sup>+</sup>CD25<sup>+</sup> regulatory cells (no. 3).



blood DCs has been observed on purified cells. Therefore, influenza virus infection triggers an autonomous program of CK production in these cells, independently of any cell-to-cell interaction. This capacity of blood DCs could thus have been evolutionally selected to allow a rapid development of protective immune response.

## References

- Steinman RM. The dendritic cell system and its role in immunogenicity. *Annu Rev Immunol*. 1991; 9:271-296.
- Banchereau J, Steinman RM. Dendritic cells and the control of immunity. *Nature*. 1998;392:245-252.
- Shortman K, Liu YJ. Mouse and human dendritic cell subtypes. *Nat Rev Immunol*. 2002;2:151-161.
- Banchereau J, Briere F, Caux C, et al. Immunobiology of dendritic cells. *Ann Rev Immunol*. 2000; 18:767-811.
- Siegal FP, Kadowaki N, Shodell M, et al. The nature of the principal type 1 interferon-producing cells in human blood [in process citation]. *Science*. 1999;284:1835-1837.
- Weninger W, von Andrian UH. Chemokine regulation of naive T cell traffic in health and disease. *Semin Immunol*. 2003;15:257-270.
- Dieu-Nosjean MC, Vicari A, Lebecque S, Caux C. Regulation of dendritic cell trafficking: a process that involves the participation of selective chemokines. *J Leukoc Biol*. 1999;66:252-262.
- Allavena P, Sica A, Vecchi A, Locati M, Sozzani S, Mantovani A. The chemokine receptor switch paradigm and dendritic cell migration: its significance in tumor tissues. *Immunol Rev*. 2000;177: 141-149.
- Cyster JG. Chemokines and cell migration in secondary lymphoid organs. *Science*. 1999;286: 2098-2102.
- Sallusto F, Palermo B, Lenig D, et al. Distinct patterns and kinetics of chemokine production regulate dendritic cell function. *Eur J Immunol*. 1999; 29:1617-1625.
- Penna G, Vulcano M, Roncari A, Facchetti F, Sozzani S, Adorini L. Cutting edge: differential chemokine production by myeloid and plasmacytoid dendritic cells. *J Immunol*. 2002;169:6673-6676.
- Vulcano M, Struyf S, Scapini P, et al. Unique regulation of CCL18 production by maturing dendritic cells. *J Immunol*. 2003;170:3843-3849.
- Fonteneau JF, Gilliet M, Larsson M, et al. Activation of influenza virus-specific CD4<sup>+</sup> and CD8<sup>+</sup> T cells: a new role for plasmacytoid dendritic cells in adaptive immunity. *Blood*. 2003;101:3520-3526.
- Marti F, Bertran E, Lluca M, et al. Platelet factor 4 induces human natural killer cells to synthesize and release interleukin-8. *J Leukoc Biol*. 2002;72: 590-597.
- Fleischer J, Grage-Griebenow E, Kasper B, et al. Platelet factor 4 inhibits proliferation and cytokine release of activated human T cells. *J Immunol*. 2002;169:770-777.
- Xia CQ, Kao KJ. Effect of CXC chemokine platelet factor 4 on differentiation and function of monocyte-derived dendritic cells. *Int Immunol*. 2003;15:1007-1015.
- Zlotnik A, Yoshie O. Chemokines: a new classification system and their role in immunity. *Immunity*. 2000;12:121-127.
- Cook DN, Beck MA, Coffman TM, et al. Requirement of MIP-1 alpha for an inflammatory response to viral infection. *Science*. 1995;269: 1583-1585.
- Shimaoka T, Nakayama T, Kume N, et al. Cutting edge: SR-PSOX/CXC chemokine ligand 16 mediates bacterial phagocytosis by APCs through its chemokine domain. *J Immunol*. 2003;171:1647-1651.
- Matloubian M, David A, Engel S, Ryan JE, Cyster JG. A transmembrane CXC chemokine is a ligand for HIV-coreceptor Bonzo. *Nat Immunol*. 2000;1: 298-304.
- Wilbanks A, Zondlo SC, Murphy K, et al. Expression cloning of the STRL33/BONZO/TYMSTR ligand reveals elements of CC, CXC, and CX3C chemokines. *J Immunol*. 2001;166:5145-5154.
- Schaffner A, Rhyn P, Schoedon G, Schaer DJ. Regulated expression of platelet factor 4 in human monocytes: role of PARs as a quantitatively important monocyte activation pathway. *J Leukoc Biol*. 2005;78:202-209.
- Scimone ML, Lutzky VP, Zittermann SI, et al. Migration of polymorphonuclear leukocytes is influenced by dendritic cells. *Immunology*. 2005;114: 375-385.
- Sallusto F, Lenig D, Mackay CR, Lanzavecchia A. Flexible programs of chemokine receptor expression on human polarized T helper 1 and 2 lymphocytes. *J Exp Med*. 1998;187:875-883.
- Yoshida R, Imai T, Hieshima K, et al. Molecular cloning of a novel human CC chemokine EBI1-ligand chemokine that is a specific functional ligand for EBI1, CCR7. *J Biol Chem*. 1997;272: 13803-13809.
- Ngo VN, Tang HL, Cyster JG. Epstein-Barr virus-induced molecule 1 ligand chemokine is expressed by dendritic cells in lymphoid tissues and strongly attracts naive T cells and activated B cells. *J Exp Med*. 1998;188:181-191.
- Kim CH, Pelus LM, White JR, Applebaum E, Johnson K, Broxmeyer HE. CK beta-11/macrophage inflammatory protein-3 beta/EBI1-ligand chemokine is an efficacious chemoattractant for T and B cells. *J Immunol*. 1998;160:2418-2424.
- Sozzani S, Allavena P, D'Amico G, et al. Differential regulation of chemokine receptors during dendritic cell maturation: a model for their trafficking properties. *J Immunol*. 1998;161:1083-1086.
- Kellermann SA, Hudak S, Oldham ER, Liu YJ, McEvoy LM. The CC chemokine receptor-7 ligands 6CKine and macrophage inflammatory protein-3 beta are potent chemoattractants for in vitro- and in vivo-derived dendritic cells. *J Immunol*. 1999;162:3859-3864.
- Andrew DP, Chang MS, McNinch J, et al. STCP-1 (MDC) CC chemokine acts specifically on chronically activated Th2 lymphocytes and is produced by monocytes on stimulation with Th2 cytokines IL-4 and IL-13. *J Immunol*. 1998;161:5027-5038.
- Ansel KM, Ngo VN, Hyman PL, et al. A chemokine-driven positive feedback loop organizes lymphoid follicles. *Nature*. 2000;406:309-314.
- Schaerli P, Willmann K, Lang AB, Lipp M, Loetscher P, Moser B. CXC chemokine receptor 5 expression defines follicular homing T cells with B cell helper function. *J Exp Med*. 2000;192: 1553-1562.
- Katou F, Ohtani H, Nakayama T, Nagura H, Yoshie O, Motegi K. Differential expression of CCL19 by DC-Lamp<sup>+</sup> mature dendritic cells in human lymph node versus chronically inflamed skin. *J Pathol*. 2003;199:98-106.
- Vanbervliet B, Bendriss-Vermare N, Massacrier C, et al. The inducible CXCR3 ligands control plasmacytoid dendritic cell responsiveness to the constitutive chemokine stromal cell-derived factor 1 (SDF-1)/CXCL12. *J Exp Med*. 2003;198:823-830.
- Struyf S, Gouwy M, Dillen C, Proost P, Opdenaker G, Van Damme J. Chemokines synergize in the recruitment of circulating neutrophils into inflamed tissue. *Eur J Immunol*. 2005;35:1583-1591.
- Seet BT, McFadden G. Viral chemokine-binding proteins. *J Leukoc Biol*. 2002;72:24-34.
- Rosenkilde MM. Virus-encoded chemokine receptors: putative novel antiviral drug targets. *Neuropharmacology*. 2005;48:1-13.
- McWilliam AS, Marsh AM, Holt PG. Inflammatory infiltration of the upper airway epithelium during Sendai virus infection: involvement of epithelial dendritic cells. *J Virol*. 1997;71:226-236.